A Chromatin-associated Kinesin-related Protein Required for Normal Mitotic Chromosome Segregation in *Drosophila*

Isabel Molina,* Sigrid Baars,* Julie A. Brill,‡ Karen G. Hales,§ Margaret T. Fuller,‡§ and Pedro Ripoll*

*Centro de Biología Molecular "Severo Ochoa" Consejo Superior Investigaciones Científicas–Universidad Autónoma Madrid, Facultad de Ciencias, UAM, Cantoblanco, 28049 Madrid, Spain; and ‡Department of Developmental Biology, §Department of Genetics, Stanford University School of Medicine, Stanford, California 94305-5427

Abstract. The *tiovivo* (*tio*) gene of *Drosophila* encodes a kinesin-related protein, *KLP38B*, that colocalizes with condensed chromatin during cell division. Wild-type function of the *tio* gene product KLP38B is required for normal chromosome segregation during mitosis. Mitotic cells in *tio* larval brains displayed circular mitotic figures, increased ploidy, and abnormal anaphase figures. KLP38B mRNA is maternally provided and expressed in cells about to undergo division. We propose that KLP38B, perhaps redundantly with other chromosome-associated microtubule motor proteins, contributes to interactions between chromosome arms and microtubules important for establishing bipolar attachment of chromosomes and assembly of stable bipolar spindles.

Chromosome arms were once thought to play a passive role in mitosis, being dragged about by forces acting at the kinetochore. However, both classic observations (for review see reference 48) and recent work (21, 48) indicate that chromosome arms play an important role in bipolar spindle assembly and chromosome behavior in mitosis. DNA-coated beads incubated in a *Xenopus* egg extract can replace chromosomes in bipolar spindle assembly in vitro (21, 48), suggesting that proteins distributed along chromosome arms can interact with, stabilize, and organize microtubules in mitotic cells. The behavior of monooriented chromosomes and fragments during mitosis suggests a polar ejection force that propels chromosome arms away from spindle poles (42). Chromatid arm fragments severed from their kinetochore in prometaphase Newt lung cells were immediately ejected radially outward, away from the spindle pole (42). The polar ejection force acting on chromosome arms appears to oppose poleward forces acting via the kinetochore to keep monooriented chromosomes from approaching too close to the pole. In so doing it may increase the probability that chromosomes will capture microtubules emanating from the opposite pole and become bioriented. In addition, polar ejection forces and the tension they exert on the kinetochore–microtubule linkage may contribute to the mechanism of congression of bioriented chromosomes to the metaphase plate (for reviews see references 16, 41). Thus, polar ejection forces acting on chromosome arms appear to be a fundamental mechanism of mitosis.

The recent discovery of kinesin-related proteins on chromosome arms suggested a mechanistic basis for the polar ejection force (1, 49, 50). The effects of depletion of the chromokinesin Xklp1 from an in vitro mitotic spindle assembly assay indicated that Xklp1 acts to position chromosomes on the spindle, stabilize central spindle microtubules, and maintain spindle bipolarity (49). The *nod* gene of *Drosophila* encodes a kinesin-related protein that binds to (1, 2) and acts along (32) chromosome arms. *nod* function is required to maintain nonexchange chromosomes on the spindle during the prolonged metaphase of meiosis I in *Drosophila* females (47). Nod protein probably acts either to keep chromosomes from moving all the way to microtubule minus ends prematurely and being lost from the nascent spindle, or to maintain tension on the kinetochore–microtubule assembly required for continued attachment of the chromosomes to the spindle. Neither of these functions is required for meiotic bivalents that have undergone exchange because the oppositely oriented homologues are held at the metaphase plate and under tension until the metaphase–anaphase transition via their physical interconnections at chiasmata. Although *Drosophila* Nod appears to contribute to the polar ejection force during female meiosis and the *nod* gene is expressed in mitotic cells (54), *nod* function is not required for normal mitotic chromosome behavior after early embryogenesis (53).

Here we report identification of mutations in a gene encoding a chromokinesin required in mitosis. The *tiovivo*

Address all correspondence to Margaret Fuller, Department of Developmental Biology, Beckman Center B300, Stanford University School of Medicine, Stanford, CA 94305-5427. Tel.: (650) 725-7681. Fax: (650) 725-7739. E-mail: fuller@cmgm.stanford.edu

(*tio*)[1] gene of *Drosophila* encodes KLP38B, a kinesin-related protein that colocalizes with condensed chromatin in mitotic cells and is required for normal chromosome segregation during mitosis. We propose that KLP38B may act, perhaps redundantly with Nod, to generate the polar ejection force in mitosis. In addition, the KLP38B chromokinesin appears to play a role in bipolar spindle assembly.

Materials and Methods

Drosophila Mutations and Culture Conditions

The *tio* gene was localized to polytene subdivision 38B, based on in situ hybridization to the ry^+ insert in the P element–induced tio^1 allele, consistent with the meiotic map position (2–54.5 map units; no recombinants between *tio* and *pr* out of 28 recombination events between *b* and *cn*) and deficiency complementation (38A6-B1; 38B6-C1, defined by the distal breakpoint of $Df(2L)TW^{161}$ and the proximal breakpoint of $Df(2L)pr^{A20}$).

Four different *tio* mutant alleles were studied: tio^1, which encodes a truncated transcript, was found during a search for mitotic mutants among a collection of P(ry^+) element–induced lethal and semilethal mutations generated by C. Berg (University of Washington, Seattle, WA), L. Cooley (Yale University, New Haven, CT), and A. Spradling (Carnegie Institute, Baltimore, MD) (11), who previously called it *sl(2)ry3*. $tio^{24\text{-}O}$ (an apparent transcriptional null) and $tio^{93\text{-}E}$ (a possible hypomorphic allele) were obtained from a collection of P(w^+) element–induced mutations generated in M. Goldberg's laboratory (Cornell University, Ithaca, NY). Excision of the tio^1 and $tio^{93\text{-}E}$ marked P elements by introduction of the *Δ2-3* source of transposase resulted in reversion to wild-type of all the mutant traits shown by homozygous individuals. The tio^{ie1} allele, an apparent transcriptional null, was recovered by imprecise excision of the tio^1 P element.

All other mutations and chromosomal rearrangements are described in reference 27, except for *T(2;3)SM5-TM6B, al² Cy lt^v cn² sp²; ss⁻ bx^{34e} e Hu Tb*, a translocation between the *SM5* and *TM6B* balancers induced by × irradiation by C. González and J. Casal (Centro de Biologia Molecular, Madrid, Spain), which was used in all crosses where homozygous *tio* larvae had to be selected.

All crosses were made at 25°C in standard *Drosophila* medium. In all cases, the multiple phenotypic traits associated with *tio* mutations varied depending on genetic background to the point that, even for transcriptionally null alleles, homozygotes vs. hemizygotes showed quantitatively different phenotypes. To minimize genetic background effects, quantitative differences between alleles were studied in hemizygotes carrying $Df(2L)pr^{A20}$, *pr cn* (38A3-4; 38B6-C1).

To quantify meiotic nondisjunction, 10 females were mated to 5 males in small vials. The parents were transferred to fresh vials every 3 d for a total period of 12 d. Progeny classes were scored every other day from eclosion until the 18th day after parents were introduced into the vial.

Cytological Analysis and In Situ Hybridization

Cytological analysis of squashed larval brains stained with aceto-orcein were carried out as in reference 20. In scoring ploidy, the number of sex chromosomes and the number of large autosomes were counted. Second and third chromosomes were not distinguished. Circular mitotic figures (CMFs) were scored as cells with chromosomes or condensed chromatin arranged in a circle around a single apparent pole. Clear cases of CMFs with chromatids (as opposed to chromosomes) oriented toward a single pole were not observed. Mitotic figures were scored as anaphases when they had two or more apparent poles with condensed chromatin oriented toward or clustered around them. In many cases, especially those with overcondensed chromatin, it was not possible to distinguish chromatids versus chromosomes. However, where they could be distinguished, it was chromatids that were oriented toward the anaphase poles.

In situ hybridization to ovaries, embryos, and testes was carried out as in reference 20, with DIG-labeled RNA probes used for embryos and ovaries and DIG-labeled DNA (Boehringer Mannheim Corp., Indianapolis, IN) probes used for hybridization to testes.

Molecular Analysis of tiovivo

The *tiovivo* locus was cloned using the P element insert in the tio^1 allele. Genomic DNA flanking the P element 3′ inverted repeat from the tio^1 allele was amplified by inverse PCR. The resulting PCR product, which contained 0.1 kb of P element DNA plus about 0.4 kb of flanking genomic DNA, was subcloned by blunt end ligation into the SmaI site in the polylinker of Bluescript KS II (Stratagene, La Jolla, CA) and used to isolate lambda EMBL3 phage carrying wild-type genomic DNA (library from J. Tamkun, UC Santa Cruz) from the region. DNA fragments representing 20 kb of genomic DNA surrounding the tio^1 insertion site were used to screen a 0–4-h embryonic cDNA library in pNB40 (N. Brown, Cambridge University, Cambridge, UK) and an adult testes cDNA library constructed in Lambda Zap II (T. Hazelrigg, Columbia University, New York). A full-length cDNA corresponding to the 3.6-kb KLP38B transcript and a full-length cDNA corresponding to the intronic 1.8-kb transcript were obtained from the 0–4-h embryonic and the testis cDNA libraries, respectively. The two full-length cDNAs were sequenced on both strands using Sequenase. Sequences were processed using the University of Wisconsin Genetics Computer Group package of sequence analysis programs (12). A third cDNA family that hybridized to the rightmost end of the cloned genomic DNA was also identified.

RNA Isolation and Northern Analysis

Total RNA was extracted from the appropriate *Drosophila* stage by the RNAzol method (TM Cinna Scientific Inc., Friendswood, TX). polyA^+ RNA was affinity purified by passage through an oligo-dT cellulose column. Northern blot analyses were carried out as described in reference 45. DNA probes were either digoxigenin-labeled by the random primed method using the DIG-DNA labeling kit (Boehringer Mannheim Corp.) or radioactively labeled by random priming. Antisense riboprobes were radioactively labeled during in vitro transcription from cDNA clones or subclones as in reference 26.

Production of Antibodies Against tio Protein

Antibodies were raised against the leu800 to gln1080 region of the nonconserved tail of KLP38B, expressed as a fusion protein in bacteria. The 3′ PstI restriction fragment (position 2398 to 3240 bp, encoding 281 amino acids) from the full-length cDNA corresponding to the 3.6-kb transcript was cloned into the PstI site of pQE10 (Qiagen, Chatsworth, CA) to produce a 6-His fusion protein (6HKLP38B). The 6HKLP38B fusion protein was prepared following the protocol of the manufacturer for purification of denatured insoluble proteins. Fusion protein was purified by binding to a Ni-NTA resin column (Qiagen) and eluted from the column at pH 5.9. Antiserum was produced by subcutaneous injection of rats with 50 μg of 6HKLP38B fusion protein at 14, 28, 49, and 84 d after the first injection.

Immunofluorescence Staining

Immunostaining of embryos was performed as in reference 20 and of testes as in reference 7. Antiserum raised against KLP38B was used at a dilution of 1:50 for embryos and 1:100 for testes. Secondary antibodies used to reveal *tio* staining were 1:200 dilutions of FITC- or RITC-conjugated goat anti–rat IgG (Jackson ImmunoResearch Laboratories, Inc., West Grove, PA). Subsequently, tubulin was detected by staining with a 1:200 dilution of YL1/2 antibody (Sera-Lab Inc., Sussex, UK), followed by a 1:400 dilution of anti–rat biotinylated secondary antibody (Amersham International, Buckinghamshire, UK), plus a 1:200 dilution of Lysamil-rhodamine-streptoavidin (Jackson ImmunoResearch Laboratories, Inc.). Alternatively, tubulin was detected simultaneously with KLP38B by staining with a 1:10 dilution of monoclonal antitubulin antibody 3A5 (38) followed by a 1:200 dilution of an anti–mouse RITC-conjugated secondary antibody (Jackson ImmunoResearch Laboratories, Inc.). Immunofluorescence staining of larval brains was performed as in reference 20, using a 1:1,000 dilution of affinity purified anticentrosomin rabbit polyclonal antibody provided by K. Li and T. Kaufman (23) and visualized with a 1:200 dilution of Cy5-conjugated anti–rabbit secondary antibody (Jackson ImmunoResearch Laboratories, Inc.). DNA was stained with propidium iodide after RNase treatment. Immunofluorescence staining was analyzed with a laser scanning confocal microscope (Carl Zeiss, Inc., Thornwood, NY). Dual color overlays and composites of confocal and conventional images were prepared using Adobe Photoshop (San Jose, CA).

1. *Abbreviations used in this paper*: CMF, circular mitotic figure; *tio*, *tiovivo*.

Results

tiovivo Is Required for Normal Mitotic Chromosome Segregation

Mutations in *tio* cause abnormal chromosome behavior and segregation in dividing larval neuroblasts (Fig. 1). For hemizygotes and all interallelic combinations of the four different *tio* alleles studied, squashed preparations of larval brains stained with aceto-orcein showed abnormal mitotic figures, indicating a requirement for tio^{+} activity for normal cell division (Table I). A total of 1,918 mitotic figures from homozygous and hemizygous mutant brains were scored quantitatively, and many more were examined for mitotic phenotypes. Mitotic larval neuroblasts in *tio* frequently (22% of 1,918 mitoses scored quantitatively) had CMFs, with sex chromosomes and major autosomes arranged in a circle, centromeres pointing inwards, and the small fourth chromosomes toward the center (Fig. 1, *C*, *F*, and *G*). Polyploid figures were common (Fig. 1, *E–G*): 26% of CMFs and cells in metaphase were aneuploid or polyploid. For many of these, the number of sex chromosomes plus major autosomes was a multiple of the haploid complement of 3. However, in a significant fraction, the number of sex chromosomes plus major autosomes departed by one or two chromosomes from the true polyploid number. For example, of 40 approximately tetraploid cells picked at random from orcein-stained squashed preparations of *tio* mutant larval brains, 38 were 4N and 2 were 4N-1. Of 419 poly- or quasipolyploid *tio* cells scored, 47% appeared tetraploid and 4% appeared octoploid, suggesting either failure of chromosome segregation or failure of cytokinesis. However, intermediate levels of ploidy were also observed: 22% of the poly- or quasipolyploid *tio* cells scored had an approximately triploid number of sex chromosomes plus major autosomes, 5% appeared pentaploid, and 10% appeared hexaploid. 12% had more than 24 large chromosomes. Some cells were clearly aneuploid (Fig. 1 *D*, for example), indicating missegregation of chromosomes as well as failure of chromosome segregation or cytokinesis. Gross aneuploidy was occasionally observed.

The extent of chromosome condensation in *tio* mitotic figures usually appeared normal. However, in 14% of metaphase figures scored, chromosomes were overcondensed, indicating metaphase arrest (29). All cells showing overcondensed metaphase chromosomes were highly polyploid, but not all highly polyploid figures had overcondensed chromosomes. The mitotic index and anaphase/metaphase ratio in *tio* brains were close to normal (Table I), indicating that most dividing cells progressed through mitosis with relatively normal timing.

Anaphase figures were frequently abnormal (38% of 306 anaphases scored). Anaphase figures were often asymmetric, with chromatids arranged in a circle at one or both poles. Euploid or polyploid bipolar anaphase figures fre-

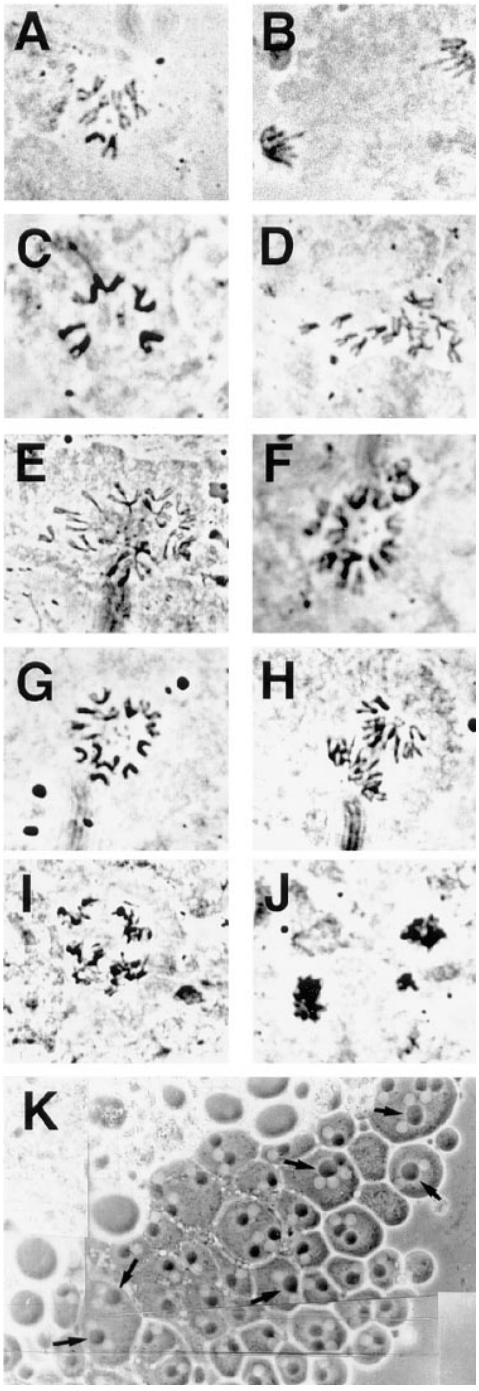

Figure 1. Mitotic figures in orcein-stained larval neuroblasts from (*A* and *B*) *tio*/+ normal and (*C–J*) *tio* mutant showing the *tio* mitotic phenotype. The appearance of mitotic figures was similar for all four *tio* alleles examined, whether hemi- or homozygous. (*A*) Normal metaphase from *tio*/+. (*B*) Normal anaphase from *tio*/+. (*C*) Diploid male mitotic figure from *tio* showing circular configuration. Note the small fourth chromosomes located in the middle of the circle and the bigger autosomes plus sex chromosomes arranged with their centromeres pointing inward and chromatid arms pointing outward. (*D*) Aneuploid metaphase figure with five X chromosomes and six major autosomes. (*E*) Octoploid metaphase. (*F*) Tetraploid circular mitotic figure. (*G*) Pentaploid circular mitotic figure. (*H*) Bipolar aneuploid anaphase in *tio*. (*I*) Tetrapolar *tio* anaphase. (*J*) Circular anaphase in *tio*. Small third cluster of condensed chromatin could be either laggards or chromatids/chromosomes oriented toward a third pole. (*K*) Live squashed testis preparation from a hemizygous $tio^{93\text{-}E}$ male showing part of a cyst of onion stage early spermatids. (*Arrows*) Spermatids with a large mitochondrial derivative associated with two nuclei of normal size.

Table I. Quantification of the Mitotic Phenotype in tio Hemizygous Neuroblasts

	wt	*tio^{1}/Df*	*$tio^{24\text{-}0}$/Df*	*$tio^{93\text{-}E}$/Df*
Fields	800	250	230	235
M.I.	0.83 ($n = 669$)	0.76 ($n = 191$)	1.03 ($n = 237$)	1.46 ($n = 343$)
A/M	0.25	0.19	0.19	0.23
Percent polyploidy	0	31.25	30	26
Percent CMF	0	14	18	30
Percent cM	0	16	15	12.3
Percent abnormal anaphases	0	35.5	32	32

Orcein-stained squashed preparations of third instar larval brains were scored for mitotic figures. A total of 771 mitotic figures in brains from hemizygous mutant larvae of the indicated genotypes and a total of 669 mitotic figures from wild-type larval brains were scored quantitatively for this table. The mitotic phenotypes of *tio^{1}*, *$tio^{24\text{-}0}$*, and *tio^{ie1}* hemizygotes waere similar for most parameters measured. *M.I.*, mitotic index measured as the number of mitotic figures per microscopic field as described in (González et al., 1988). *n*, number of mitotic figures analyzed in each experiment. *A/M*, ratio of anaphase to metaphase figures. CMFs were considered metaphases for the purposes of this table and were included in the total represented by M to arrive at the A/M ratio. *cM*, metaphase figures resembling those found after long colchicine treatment. *abnormal anaphases*, anaphase figures showing abnormalities such as broad poles, disoriented chromatids, asymmetrical numbers of chromatids going to the two poles, etc.

quently had broad poles (Fig. 1 *H*). Tripolar and tetrapolar anaphases were found (Fig. 1, *I* and *J*), but rarely. Binucleate cells were also occasionally observed in *tio* brain squashes (data not shown).

Staining of *tio/Df* larval brains with propidium iodide and anticentrosomin revealed a variety of defects in chromosome and centrosome arrangement and number (Fig. 2), reflecting the range of mitotic defects observed in orcein-stained squashed preparations. Many mitotic figures appeared normal (Fig. 2, *A* and *B*). In a random sample of 49 cells in prometaphase, metaphase, or anaphase from *tio^{1}/Df* (25 cells) or *$tio^{24\text{-}0}$/Df* (24 cells), larval brains stained for immunofluorescence in two different experiments, roughly half (63%) had no apparent defects. However, cells with clearly abnormal numbers and arrangements of chromosomes and centrosomes were common (37%). Defects observed ranged from circular arrays of chromosomes surrounding a single centrosomal mass (6%) (Fig. 2 *C*), consistent with failure of centrosome separation, to cells with two separated centrosomes but defects in chromosome number (Fig. 2 *E*) or arrangement (Fig. 2 *F*) (25%). In some cases (roughly 6% of mitotic figures scored), cells appeared to have some chromosomes aligned at a metaphase plate while other chromosomes in the same cell appeared clustered around only one of the two separated centrosomes (Fig. 2 *D*), suggesting defects in the ability of chromosomes to form bipolar attachments to the spindle rather than defects in centrosome separation. Some cells (6%) had more than two well-separated centrosomes (Fig. 2 *H*, 4 centrosomes; Fig. 2 *G*, 8 centrosomes: 5 are visible, and 3 more were out of the plane of focus). As in quantitating the cells in mitosis, we only counted those with large centrosomes and clear, well-condensed chromosomes, so the frequency of abnormal mitotic figures may have been underestimated. This is especially true for cells with a single centrosomal mass where chromosomes may have been either poorly condensed or too closely massed to be clearly distinguished (compare 6% to the frequency of CMFs in Table I).

tio males had mild meiotic defects. *$B^{S}Y$*; *tio^{1}/tio^{1}* males showed a weak but significant ($P < 0.002$) increase in sex chromosome nondisjunction (0.42% out of 2,864 progeny scored) compared with control *$B^{S}Y$*; *tio^{1}/CyO* males (0.19% out of 1,612 progeny scored). Other *tio* alleles tested were male sterile. Early spermatids in *tio* males occasionally showed variation in nuclear size, indicating defects in meiotic chromosome disjunction (8), or were binucleate, indicating karyokinesis without cytokinesis (Fig. 1 *K*, *arrows*).

Relative viability of *tio* hemizygotes compared with heterozygous siblings ranged from 0 to as high as 80%, depending on genetic background and culture conditions. *tio* adults had visible defects often associated with mitotic mutants, including rough eyes and bristle abnormalities. *tio* adults showed behavioral defects including held up wings, delay in or failure to mate, and retention of fertilized eggs. Females often had one or both ovaries rudimentary. Animals lacking both maternal and zygotic *tio* function died as mature embryos without strong or consistent pattern defects. Of about 100 mature embryos from *tio^{1}/Df* females mated to *tio^{1}/CyO* males, only one with defective segmentation and two with general cuticle defects were observed. Head involution defects were more common but less frequent than the expected number of homozygous embryos. Of 300 midstage embryos produced from a similar cross, only two showed gross abnormalities (lack of anterior segments during germ band elongation). The relative viability of homo- or hemizygous mothers did not noticeably affect the phenotype or viability of their offspring. Animals lacking the maternal *tio* contribution but carrying a paternally contributed wild-type *tio* allele were viable and appeared normal.

tiovivo Encodes Kinesin-like Protein KLP38B

Over 20 kb of wild-type genomic DNA surrounding the insertion site of the *tio^{1}* allele was cloned (Fig. 3 *A*) (Materials and Methods). Northern blots probed with fragments of the cloned DNA revealed that the *tio* region encodes two transcripts (Fig. 3): a 3.6-kb transcript abundant in 0–2 h embryos and present in later embryos and adults (Fig. 3 *B*) and a 1.8-kb transcript, abundant in 4–8-hour embryos and present in later embryos and adults (Fig. 3 *B*). Full-length cDNAs corresponding to the 3.6- and 1.8-kb transcripts from the region flanking the *tio^{1}* insert were isolated (Materials and Methods) and hybridized to Southern blots of the digested genomic phage clones to determine the arrangement of exons and introns in the region (Fig. 3 *A*). In addition, the sequences of the cDNAs were compared with a sequence of genomic DNA across the region kindly provided by D. Ruden. The 3.6-kb transcript derived from

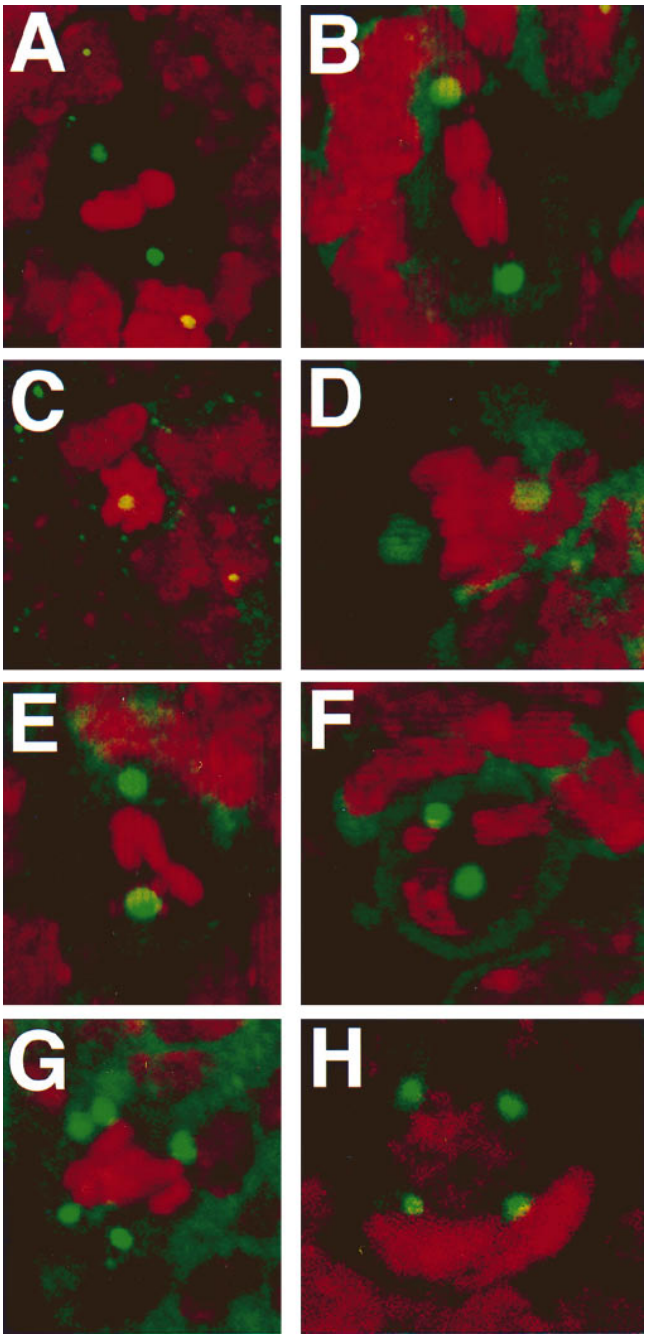

Figure 2. *tio* mutant animals exhibit a variety of defects in the arrangement of chromosomes and centrosomes in mitosis. Confocal fluorescence micrographs of larval brains from tio^{1}/Df (*B* and *D–F*) or $tio^{24\text{-}0}/Df$ (*A*, *C*, *G*, and *H*) mutant animals stained with anticentrosomin to reveal centrosomes (*green*) and propidium iodide to reveal chromosomes (*red*). (*A*) Phenotypically normal metaphase. (*B*) Phenotypically normal early anaphase. Note that the two fourth chromosomes are closest to the poles. (*C*) CMF. Chromosomes arranged in a circle around a single centrosome. (*D*) Abnormal metaphase. Cell with a subset of chromosomes aligned along the metaphase plate and a group of apparently monooriented chromosomes associated with the centrosome at right. (*E*) Abnormal mitotic cell with three fourth chromosomes associated with the lower centrosome and only a few large chromosomes. (*F*) Mitotic cell with abnormal arrangement of chromosomes. (*G*) Polyploid mitotic cell with eight centrosomes (three are out of the plane of focus). (*H*) Mitotic cell with four centrosomes.

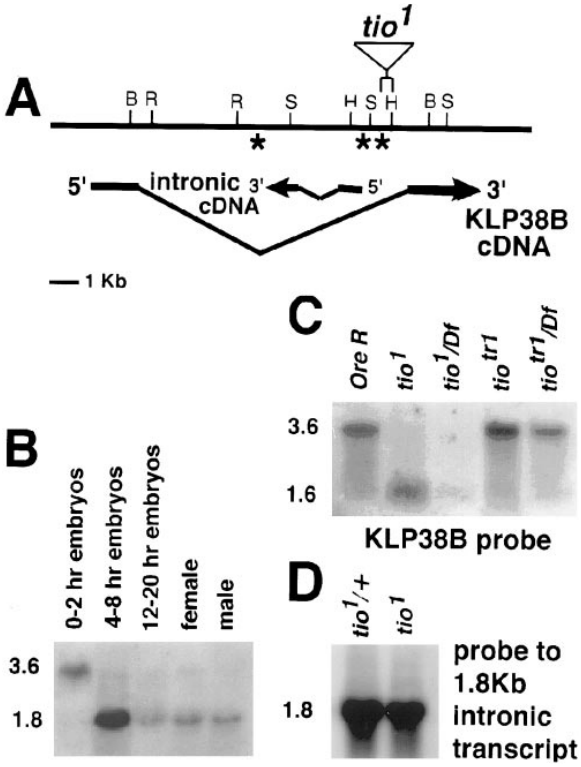

Figure 3. Molecular organization of the *tio* gene. (*A*) Top line: Restriction map of the 20 kb of genomic DNA containing *tio*. Lower lines: Exon/intron map of the 3.6-kb KLP38B transcript and the 1.8-kb transcript contained within its large intron. The tio^{1} P element is inserted within the intron of the 3.6-kb transcript, in a 700-bp PvuII-HindIII fragment upstream of the 5′ end of the cDNA representing the 1.8-kb transcript. The $tio^{24\text{-}0}$ (*) and $tio^{93\text{-}E}$ (**) inserts were mapped to the intron of the 3.6-kb transcript by Alphey et al. (3), roughly as shown by the asterisks. The exact relationship of the $tio^{24\text{-}0}$ and $tio^{93\text{-}E}$ inserts to the position of the intronic transcript was not published in Alphey et al. (3). (*B*) Developmental Northern probed with a cloned genomic fragment showing the two transcripts (3.6 and 1.8 kb) derived from the genomic DNA flanking the tio^{1} P element insert. Both transcripts were present in all stages studied, although the 3.6-kb transcript was more abundant in 0–2-h embryos and the 1.8-kb transcript was more abundant in 4–8-h embryos. (*C* and *D*) Northern analysis of polyA^{+} RNA from third instar larvae of the indicated genotypes hybridized with (*C*) a DIG-labeled 5′ fragment from the KLP38B cDNA or (*D*) an antisense riboprobe generated from the cDNA representing the 1.8-kb transcript. Note that in *C*, instead of the wild-type 3.6-kb transcript, a truncated 1.6-kb transcript appeared in tio^{1} homo- or hemizygotes. The transcript returned to normal size in larvae homo- or hemizygous for tio^{tr1}, a transposase-induced true revertant of tio^{1}. In contrast, no change was observed in the 1.8-kb transcript in tio^{1} animals (*D*).

two exons separated by an 11-kb intron (Fig. 3 *A*). The oppositely oriented 1.8-kb transcript also derived from two exons, located within the large intron of the 3.6-kb transcript (Fig. 3 *A*). The P element responsible for the tio^{1} mutation was inserted within the large intron of the 3.6-kb transcript and just 5′ of the 1.8-kb transcript (Fig. 3 *A*). Sequence analysis of a full-length cDNA representing the 1.8-kb transcript showed only short open reading frames

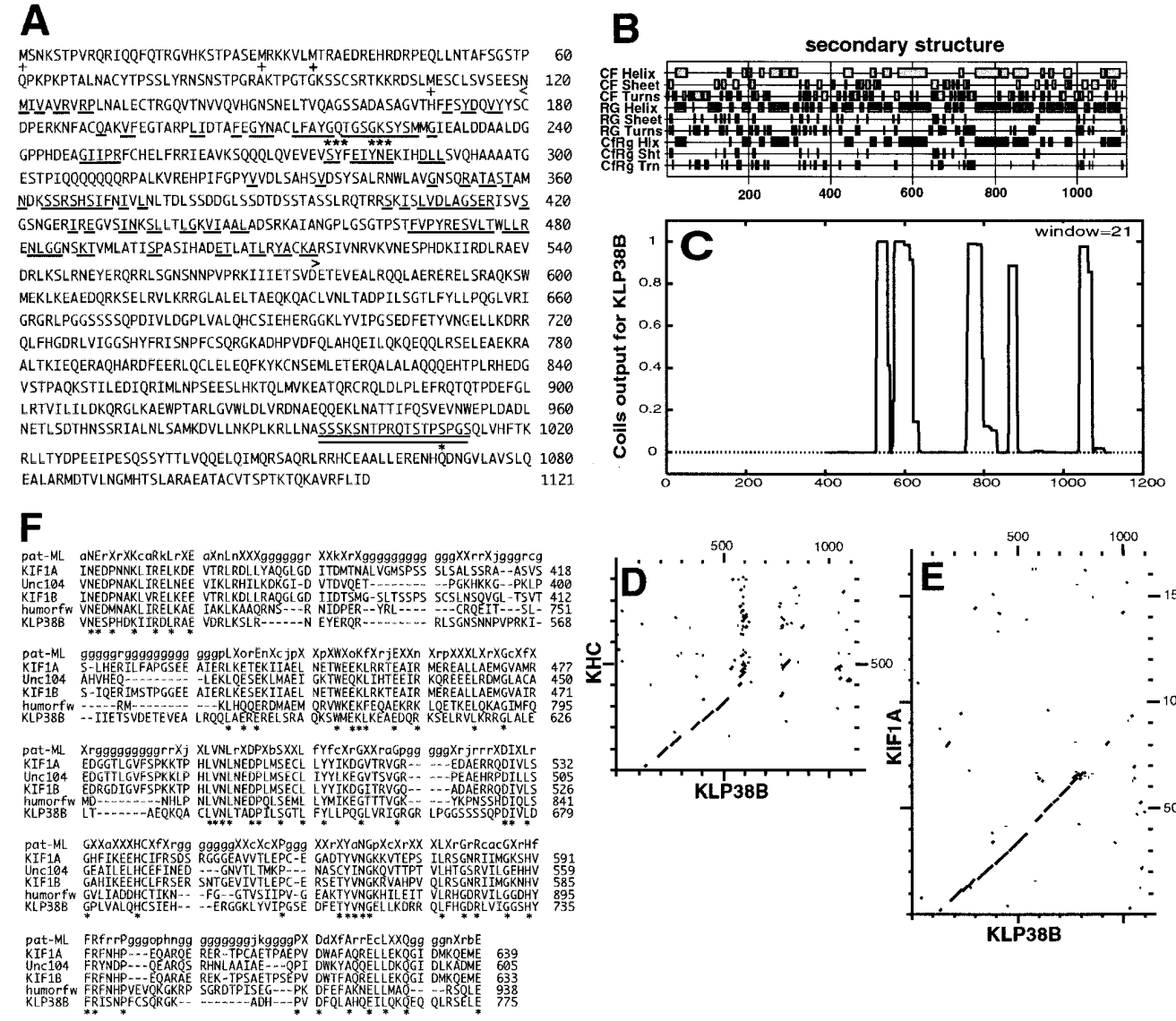

Figure 4. tio encodes a kinesin-like protein of the Unc104/KIF1A/KIF1B family. (*A*) Predicted sequence of the KLP38B protein. (+) Possible initiator methionine residues. The first methionine was taken as the start in assigning residue numbers. A predicted kinesin-like motor domain extends from approximately amino acid 120 (<) to approximately amino acid 115 (>). Single underlined residues are similar or identical to the conserved amino acid motifs characteristic of members of the kinesin-like protein superfamily as denoted in reference 44. (***) P-loop residues comprising part of the nucleotide binding motif. The region from amino acid 996 to 1013 (*double underline*) is similar in organization to the DNA binding region of a number of proteins that bind AT-rich DNA (10). This region also includes a predicted phosphorylation site for *cdc2*. (*). (*B*) Predicted KLP38B secondary structure. Note predicted α-helical regions centered on residues 600 and 800, near the beginning and the end of the stalk. (*C*) Plot of probability of coiled coil regions in KLP38B predicted by the method of reference 28. Regions likely to form coiled coils lie near the beginning and end of the stalk. (*D*) Dot matrix comparison of KLP38B and the *Drosophila* kinesin heavy chain. Diagonal line highlights the homology to the KHC motor domain. (*E*) Dot matrix comparison of KLP38B and the mouse KIF1A protein. Diagonal line highlights the predicted motor domain homology plus a region of extended homology in the stalk region. Dot matrix plots were prepared using the COMPARE (Window: 30, Stringency: 20) and DOTPLOT programs of University of Wisconsin Genetics Computer Group. (*F*) Multiple sequence alignment (PIMA) of stalk regions of KLP38B, KIF1A (gi|976235), Unc104 (gi|102551), KIF1B (gi|1083399), and *humorfw* (gi|452517), showing patches of sequence conservation across several members of the Unc104 subfamily of kinesin-related proteins. (*) Residues in KLP38B that are identical in three of the four other proteins.

and no significant homology with nucleic acid or protein sequences in GenBank.

Analysis of transcripts in *tio* mutants using cDNA-specific probes indicated that the 3.6-kb transcript corresponds to the *tio* gene product. The 3.6-kb transcript was truncated to 1.6 kb in *tio*^{1} and returned to normal size upon reversion of the *tio*^{1} mutation to wild type with transposase (Fig. 3 *C*), while the size of the 1.8-kb transcript was not altered in the *tio*^{1} P element–induced allele (Fig. 3 *D*). In situ hybridization to testes showed that message

corresponding to the 3.6-kb transcript was reduced in level in testes from $tio^{93\text{-}E}$ and not detected with either a 5′ or 3′ exon probe in testis from $tio^{24\text{-}O}$ or tio^{ie1} hemizygotes (data not shown), indicating that the latter are likely to be null alleles.

The 3.6-kb *tio* transcript encodes a predicted protein belonging to the kinesin heavy chain superfamily (Fig. 4). A gene in polytene interval 38B encoding a kinesin-like protein (KLP38B) had been predicted (13). To confirm that *tio* encodes KLP38B, we showed that an EMS-induced mutation, kindly provided by D. Ruden and shown by him to cause a stop codon at amino acid residue 760 (43), near the end of the predicted stalk region of KLP38B (see below), failed to complement and showed the characteristic mitotic defects in trans to the P element–induced *tio* alleles in our study. The predicted protein encoded by the *tio* open reading frame is 1,121 amino acids long starting from the first in frame methionine. However, the protein could start at a methionine 28, 34, or even 108 amino acid residues downstream (Fig. 4 *A*). None of these potential start codons occur in a nucleic acid sequence context that strongly matches the consensus for *Drosophila* translation starts (9).

The predicted KLP38B protein has a characteristic kinesin-like motor domain near but not at its NH_2 terminus (Fig. 4, *A* and *D*), suggesting action as a microtubule motor (31). The motor domain is followed by a stalk region (residues 524–775 of KLP38B) containing patches of significant homology with analogous regions of members of the Unc104 subfamily of kinesin-related proteins (Fig. 4, *E* and *F*), including KIF1A and KIF1B, kinesin-related proteins associated with synaptic vesicles or mitochondria, respectively (33, 37). KLP38B had the highest overall homology with *humorfw*, encoded by a cDNA cloned from a rapidly dividing human myeloid cell line (35). The stalk region of KLP38B has two clusters of residues predicted to participate in α-helix and/or coiled coil formation near its beginning and end (Fig. 4, *B* and *C*). The stalk region of KLP38B is followed by a COOH-terminal tail domain including a region (Ser996 to Ser1013) with an arrangement of prolines, serines, and basic amino acids resembling the DNA binding motifs of several proteins that bind to AT-rich DNA, including HMG 1 (10).

The KLP38B gene is expressed in mitotically cycling cells. KLP38B mRNA was abundant (Fig. 3 *B*) and uniformly distributed (data not shown) in preblastoderm embryos, present in the stereotyped premitotic spatio-temporal domains (15) during cycle 14, became restricted to nervous tissue during mid-embryogenesis, and was detected only in the procephalic lobe neuroblasts and nerve cord in late embryos (Fig. 5). KLP38B mRNA was expressed in mitotically active regions in larval brains and imaginal discs (data not shown). In stage 5 and later egg chambers, KLP38B mRNA was detected both in follicle and nurse cells (Fig. 5 *C*) and generally appeared uniform in the oocyte cytoplasm. In wild-type adult testes, KLP38B transcript was detected only in the mitotically active gonial cells (Fig. 5 *D*, *arrowheads*) and mature primary spermatocytes (Fig. 5 *D*, *arrows*). A 5′ exon probe but not a 3′ exon probe detected the KLP38B transcript in tio^{1} testes, indicating that the truncated message encoded by the tio^{1} allele (Fig. 3 *C*) could encode a product containing the motor domain but lacking the COOH-terminal tail.

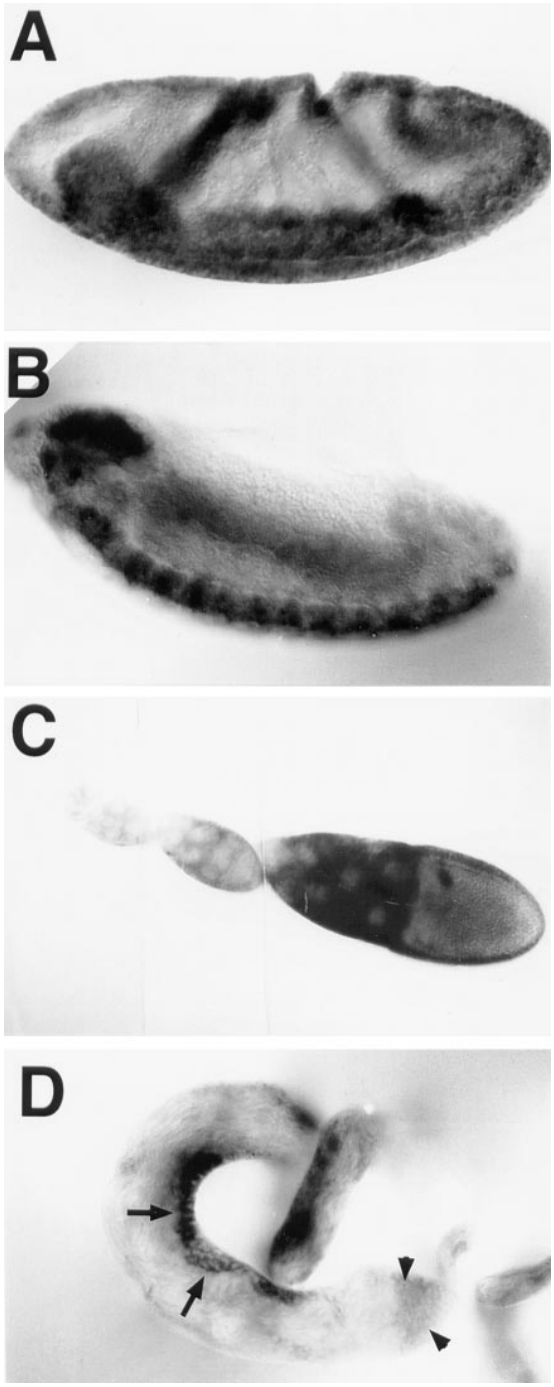

Figure 5. Transcription pattern of *tio* in wild-type embryos, ovaries, and testes. Whole mount in situ hybridizations with a 5′ exon probe. (*A*) Stage 10 embryo showing high levels of *tio* transcript in regions corresponding to mitotic domains 1, 2, 3, 4, and 10 of cycle 14. (*B*) Germ band retracted embryo showing *tio* transcript accumulation in the nerve cord and the procephalic lobe neuroblast region. (*C*) Ovariole showing accumulation of *tio* transcript in follicle and nurse cells from stage 5 of oogenesis. *tio* RNA was not detected in the germarium. (*D*) Adult testis showing accumulation of *tio* transcript in the mitotically active gonial cells (*arrowheads*) and in primary spermatocytes just about to enter meiotic division (*arrows*).

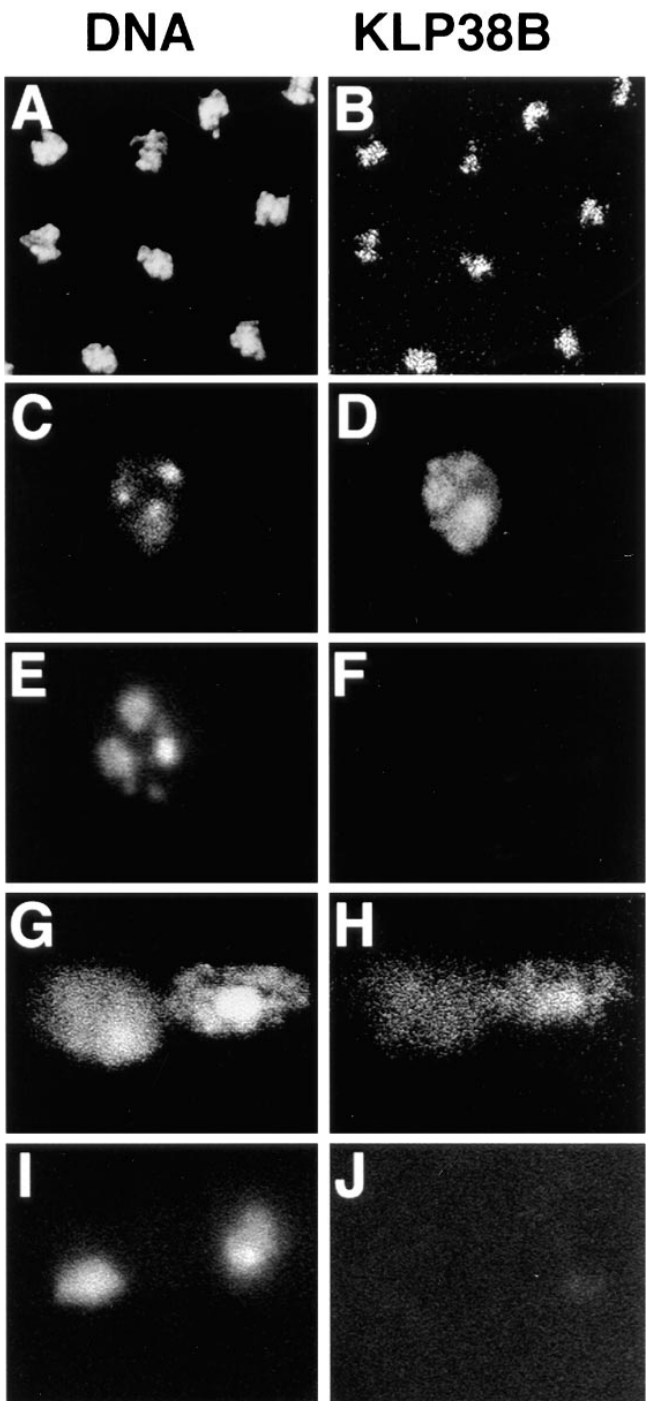

Figure 6. The KLP38B protein encoded by *tio* localizes to mitotic and male meiotic chromosomes. Confocal immunofluorescence microscope images of embryos or testes costained for DNA with propidium iodide and KLP38B with anti-KLP38B antibody. (*A* and *B*) Low-magnification view of metaphase figures at the surface of a syncytial blastoderm embryo. (*A*) DNA and (*B*) KLP38B colocalized. (*C* and *D*) Clustered meiotic bivalents in a metaphase I *Oregon R* spermatocyte showing colocalization of (*C*) chromatin and (*D*) KLP38B. *C* and *D* show the same field. (*E* and *F*) KLP38B was not detected on metaphase I bivalents from (*F*) tio^{1} or $tio^{24\text{-}0}$ (data not shown) males. *E* and *F* show same field stained for (*E*) DNA and (*F*) KLP38B. (*G* and *H*) Early anaphase I meiotic chromosomes from *Oregon R* testis, showing colocalization of (*G*) chromatin and (*H*) KLP38B. *G* and *H* show the same field. (*I* and *J*) KLP38B was not detected on anaphase I bivalents from tio^{1} males. *I* and *J* show same field stained for (*I*) DNA and (*J*) KLP38B with anaphase I chromosomes at a later stage than in *G* and *H*.

The tiovivo Protein KLP38B Colocalizes with Condensed Chromatin during Mitosis and Male Meiosis

The KLP38B protein colocalized with condensed chromatin during both mitosis and male meiosis (Fig. 6). Antibodies raised against a 281–amino acid fragment from the nonconserved region of the KLP38B tail (Materials and Methods) stained mitotic chromosomes at metaphase (Fig. 6, *A* and *B*) and anaphase and nuclei at telophase (data not shown) in both syncytial blastoderm and cycle 14 embryos. The anti-KLP38B antibodies also stained metaphase (Fig. 6, *C* and *D*) and anaphase (Fig. 6, *G* and *H*) chromosomes during male meiosis. The antigen did not appear to be localized only to centromeres, but rather colocalized with the mass of condensed chromatin as detected by propidium iodide staining.

The chromosomal staining observed was due to the presence of the *tio* gene product, as the antigen was not detected on meiotic chromosomes in males homozygous for tio^{1} (which presumably encodes a truncated product lacking the epitope against which the antibody was raised) (Fig. 6, *E* and *F*, and *I* and *J*) or $tio^{24\text{-}0}$ (a transcriptional null) (data not shown), demonstrating the specificity of the antibody staining detected by immunofluorescence. Immunofluorescence staining of embryos with the preimmune serum showed only background staining (data not shown).

Double-label immunofluorescence staining of syncytial and cellular blastoderm embryos with antitubulin and anti-KLP38B indicated that KLP38B was localized to the positions where the chromosomes lie at metaphase, anaphase, and telophase (Fig. 7), rather than to spindle fibers. KLP38B did not appear to localize to mitotic spindles, with the possible exception of a region where microtubules overlapped chromosomes at microtubule plus ends (for example, Fig. 7, *E* and *F*). Anti-KLP38B staining localized to centrosomes or the midbody was never observed.

Detection of KLP38B at the position of chromosomes was cell cycle dependent. In cycle 14 embryos, antibody staining was only detected in the mitotic domains. No localized staining was detected in interphase cells (Fig. 7 *G*), suggesting that KLP38B could be either dispersed or degraded during interphase.

Discussion

The *tiovivo* gene of *Drosophila*, required for normal chromosome segregation during mitosis, encodes kinesin-related protein KLP38B. Six lines of evidence indicate that mutations in the KLP38B gene rather than the gene encoding the 1.8-kb transcript derived from the large intron of KLP38B are responsible for the mitotic and visible phenotypes associated with *tio* mutants. (*a*) The KLP38B message is truncated in the P element–induced tio^{1} allele but restored to normal size when the mutation is reverted to wild type, while there was no alteration in size in the 1.8-kb transcript in the same mutant (Fig. 3). (*b*) Antibodies against the COOH-terminal tail of KLP38B stain meiotic

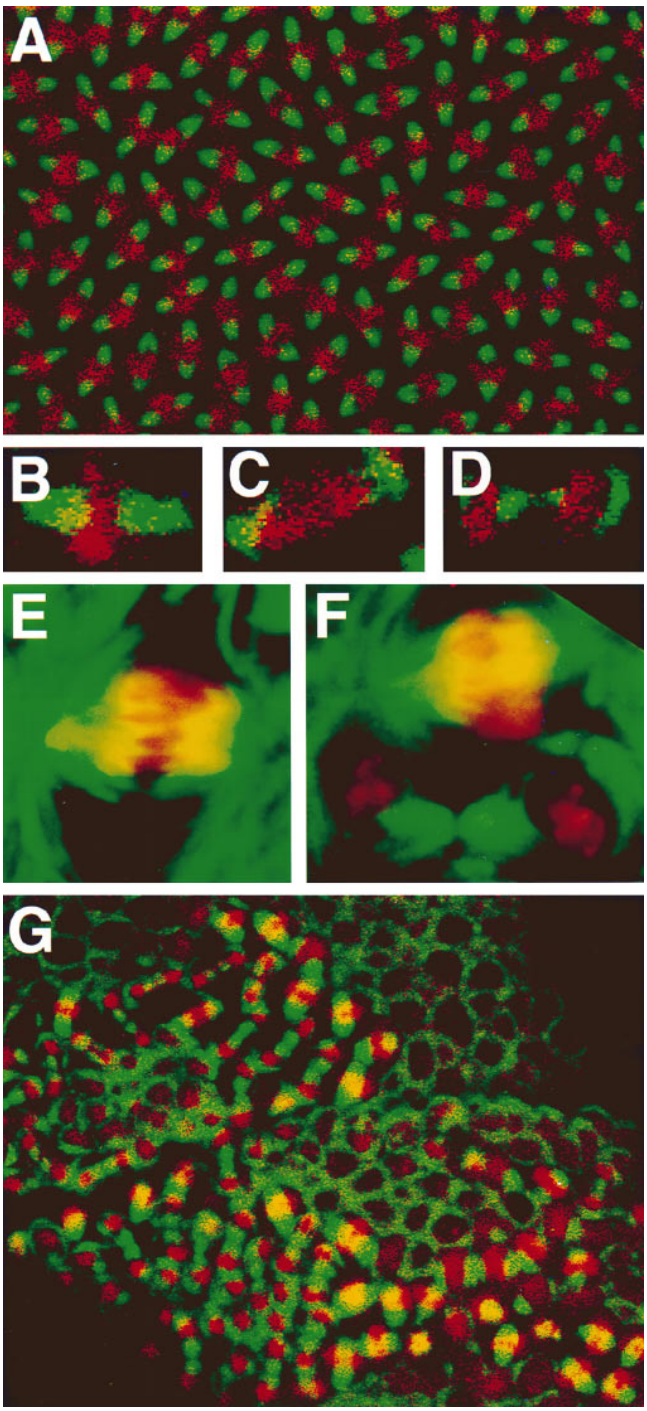

Figure 7. Localization of KLP38B does not correspond to spindle fibers and is cell cycle dependent. (*A*) Surface view of a cycle 13 embryo showing a field of metaphase spindles (microtubules in *green*) with KLP38B (*red*) localized to the metaphase plate. (*B–D*) Higher-magnification views showing localization of KLP38B (*red*) with respect to spindle microtubules (*green*) during mitosis in syncytial blastoderm embryos. (*B*) Metaphase: microtubules form a bipolar spindle that is not decorated with anti-KLP38B. Instead, KLP38B localizes to the region of the metaphase plate. (*C*) Anaphase: KLP38B staining splits into two parts that are now located closer to the poles, reminiscent of the position of early anaphase chromatids. (*D*) Late anaphase: the central spindle (*green*) can be clearly detected and does not appear to contain appreciable concentrations of KLP38B. KLP38B (*red*) is located nearer to the poles, in the region that would be occupied by the chromatids. (*E* and *F*) Higher-magnification views of cells in (*E*) metaphase and (*F*) metaphase (*top*) and telophase (*bottom*) from a gastrulating cycle 14 embryo stained for microtubules (*green*) and KLP38B (*red*), showing KLP38B at the position that is normally occupied by the metaphase and telophase chromatin. (*G*) Localization of KLP38B was cell cycle dependent. Low-magnification surface view of a gastrulating cycle 14 embryo stained for microtubules (*green*) and KLP38B (*red*) showing mitotic domains 5 and 6. Note that while KLP38B (*red*) was easily detected in cells undergoing mitosis, little or no localized KLP38B was detected in interphase cells.

chromatin in wild-type testes, but not in testes mutant for the two different *tio* alleles tested (Fig. 6). Furthermore, in situ hybridization with a KLP38B probe showed reduced or absent mRNA in testes from at least three different *tio* alleles. (*c*) A nonsense mutation in the KLP38B coding region fails to complement the P element–induced alleles used in this study for the characteristic *tio* mitotic defects. (*d*) Injection of antibodies against KLP38B into wild-type syncytial blastoderm embryos resulted in formation of circular mitotic figures (43) reminiscent of the mitotic abnormalities observed in *tio* mutant larval brains in our study. (*e*) Expression of the KLP38B cDNA under control of the *hsp26* promoter but without induction by heat shock rescued the sterile and partially rescued the visible phenotypes associated with the mutants (3). (*f*) A 10-kb fragment of genomic DNA containing the KLP38B large intron restored normal levels of the 1.8-kb transcript but did not rescue the cytokinesis or adult morphological defects associated with a P element–induced mutation that affected KLP38B expression when introduced into flies by P element–mediated germ line transformation (36).

KLP38B protein is associated with condensed chromatin during mitosis. Although direct binding to DNA has not yet been tested, KLP38B, like other members of the chromokinesin family of kinesin-like proteins proposed by Vernós and Karsenti (48), could associate with condensed chromatin directly via a possible DNA binding motif in its COOH-terminal cargo domain. The possible DNA binding motif of KLP38B contains a predicted *cdc2* phosphorylation site (34) at Ser1010, suggesting that cell cycle–dependent association of KLP38B protein with chromatin might be regulated by phosphorylation. Indeed, L. Alphey and co-workers (3) have demonstrated physical interaction between KLP38B and PP187B, a phosphatase involved in mitosis in *Drosophila* (4). As KLP38B transcripts accumulate in cells about to enter mitosis or meiosis, the protein could be degraded after telophase and synthesized de novo before the next cell division.

Role of the KLP38B Chromokinesin in Mitosis

Lack of KLP38B function leads to a variety of mitotic defects, including aneuploid and polyploid cells, asymmetric metaphase and anaphase figures with abnormal arrangements of chromatin, and a high frequency of CMFs resembling the array of monooriented chromosomes around monopoles in newt lung cells (5) and several other *Drosophila* mitotic mutants (18, 19, 22, 46). Cells where chromosomes remain in a circular array around a single cen-

trosomal mass (as in Fig. 2 *C*) would be unlikely to undergo cytokinesis, contributing to the observed high incidence of true polyploids. Ohkura et al. also observed elevated frequencies of 4N and 8N cells in KLP38B mutants, which they attributed to failure of cytokinesis (36). However, Ohkura et al. did not observe the variety of other mitotic defects found in our study, perhaps because they characterized two hypomorphic alleles, whereas strong loss of function or null alleles were included in our study.

We propose that KLP38B protein bound to condensed chromatin facilitates interactions between chromosome arms and microtubules important for both bipolar attachment of chromosomes to the spindle and bipolar spindle assembly. The CMFs and wide range of mitotic defects characteristic of *tio* could arise from defects in both of these processes.

KLP38B could act to push chromosome arms away from spindle poles, either by coupling chromosome arms to astral microtubule dynamics or by plus end–directed microtubule motor activity. When a chromosome first captures an astral microtubule in early prometaphase, it moves rapidly toward the corresponding spindle pole (40). Loss of KLP38B function could lead to monooriented chromosomes because of insufficient antipoleward force to move chromosomes out to a position where they encounter and capture microtubules from the opposite pole. If some chromosomes are still monooriented by anaphase onset (as often occurs in cultured newt lung cells [42]), it could account for the aneuploid cells and odd levels of ploidy observed in *tio* mutants. For example, Fig. 2 *D* shows a cell in which some chromosomes are aligned at the metaphase plate while several chromosomes appear to remain monooriented toward the same pole. If such a cell were to enter anaphase, the products might be one daughter with a near triploid chromosome constitution and one daughter with fewer than the normal number of chromosomes (as in Fig. 2 *E*).

KLP38B could also act to capture and stabilize astral microtubules in the vicinity of chromatin, thereby converting a pair of asters to the classic bipolar spindle shape and stabilizing spindle bipolarity by increasing antiparallel interactions between microtubules from opposite poles. A similar role was proposed for the *Xenopus* chromokinesin XKLP1 based on in vitro studies (49).

Ability of chromokinesins to mediate interactions between chromosomes and spindle microtubules could play an integral role in the mechanism of centrosome separation. When centrosomes begin separation in prophase, each organizes an astral array of microtubules, but in many cases little or no central spindle is evident (6, 30, 39, 51). If nuclear envelope breakdown occurs before centrosomes are well separated, stabilization of microtubules extending toward the chromosomes by KLP38B and other chromokinesins would create a V-shaped microtubule array with the vertex at the chromosomes and the tips at the centrosomes, an arrangement commonly observed in *Drosophila* prometaphase neuroblasts (52). The resulting juxtaposition of microtubules from opposite poles could facilitate antiparallel interactions that help drive the poles apart, perhaps via action of bipolar complexes of other plus end–directed kinesin-related proteins such as the BIMC homologue KLP61F (14, 22, 24, 25, 52). If KLP38B mutants are deficient in ability of chromosome arms to stabilize microtubule arrays, there could be insufficient force to reliably separate spindle poles after nuclear envelope breakdown, leading to the CMFs (Fig. 1) and monopolar chromosome arrays (Fig. 2 *C*) observed in *tio* larval brains. Subsequent failure of cytokinesis would then give rise to tetra- and octoploid cells (Table I) and polyploid cells with four or eight centrosomes (Fig. 2, *G* and *H*). Whether cells form monopoles leading to true tetraploids or well-separated spindle poles with abnormally oriented chromosomes in *tio* may depend on cell-to-cell variation in the relative timing of centrosome separation and nuclear envelope breakdown.

The effects of *tio* null mutations were surprisingly mild, perhaps due in part to functional redundancy with the product(s) of similarly acting gene(s), for example *nod.* Both *tio* and *nod* encode predicted microtubule motors that bind to chromosomes. Although *nod* function is not essential for mitosis, *nod* is expressed in somatic cells and a dominant allele results in a phenotype in mitotic cells (17). If KLP38B and Nod play similar roles in mitosis, wild-type *nod* function might not be essential for viability or mitosis because KLP38B is normally sufficient. Likewise, normally cryptic function of Nod in mitotic cells may partially alleviate the effects of loss of function of KLP38B.

Much of the role played by chromosomes in assembly of a bipolar spindle can be substituted by plasmid DNA-coated beads previously equilibrated in a *Xenopus* interphase egg extract to allow the DNA to form chromatin (21). Although these beads probably lacked kinetochores, when placed into a mitotic extract they induced local assembly of microtubules, which then resolved into a fine bipolar spindle (21). Chromokinesins like KLP38B, XKLP1, and Nod are good candidates for the chromatin-associated factors that allow plasmid-coated beads to mimic chromosome arms. Thus, the properties of microtubule motors associated with chromatin, together with plus end–directed microtubule motors that cross-link and slide antiparallel microtubules and minus end–directed microtubule motors that bundle microtubule ends, can provide many of the functions essential for bipolar spindle assembly in animal cells.

We thank D. Ruden (University of Kansas), M. Goldberg, and A. Spradling for providing *tio* alleles, and L. Alphey (University of Manchester), D. Ruden, and D. Glover (University of Dundee) for communicating unpublished results. We thank K. Li and T.C. Kaufman (Indiana Univesity) for anticentrosomin antibodies and M. Scott (Stanford Univeristy, Stanford, CA) for access to a confocal microscope at Stanford. M.T. Fuller thanks L.S.B. Goldstein (University of California, San Diego) for pointing out the extended region of homology between KLP38B and KIF1A and KIF1B. The group in Madrid is indebted to A. Villasante (Madrid) for his continuous help and encouragement, N. Azpiazu, M. Calleja, I. Guerrero, and E. Sanchez-Herrero (all in Madrid) for discussions, and A. Sanchez for technical assistance.

I. Molina was supported by a Dirección General de Investigación Científica y Técnica (DGICYT) postdoctoral fellowship and a DGICYT reincorporation contract, S. Baars was supported by EU Network No. CECHRX-CT93-0186, J.A. Brill was supported by National Institutes of Health (NIH) postdoctoral Fellowship No. 5-F32-HD07728 and a Katharine D. McCormick Fellowship award, and K.G. Hales was supported by a Howard Hughes Medical Institute predoctoral fellowship. This work was supported by NIH grant No. 5R01-HD29194 to M.T. Fuller and by DGICYT grants PB90-0110 and PB93-0174 and an institutional grant from Fundacion Ramon Areces to P. Ripoli.

Received for publication 5 February 1997 and in revised form 25 September 1997.

Note Added in Proof. The sequence data for *tio*/KLP38B is available from GenBank/EMBL/DDBJ under accession number Y15427.

References

1. Afshar, K., N. Barton, R.S. Hawley, and L.S.B. Goldstein. 1995. DNA binding and meiotic chromosomal localization of the *Drosophila* NOD kinesin-like protein. *Cell*. 81:129–138.
2. Afshar, K., J. Scholey, and R.S. Hawley. 1995. Identification of the chromosome localization domain of the *Drosophila* Nod kinesin-like protein. *J. Cell Biol.* 131:833–843.
3. Alphey, L., L. Parker, G. Hawcroft, Y. Guo, K. Kaiser, and G. Morgan. 1997. KLP38B—a mitotic kinesin–related protein which binds PP1. *J. Cell Biol*. 138:395–409.
4. Axton, J.M., V. Dombradi, P.T.W. Cohen, and D.M. Glover. 1990. One of the protein phosphatase 1 isoenzymes in *Drosophila* is essential for mitosis. *Cell*. 63:33–46.
5. Bajer, A. 1982. Functional autonomy of monopolar spindle and evidence for oscillatory movement in mitosis. *J. Cell Biol.* 93:33–48.
6. Bajer, A.S., J. Mole-Bajer, M. De Brabander, J. De Mey, G. Geuens, and S. Paulaitis. 1980. Aster migration and functional autonomy of monopolar spindle. *In* Microtubules and Microtubule inhibitors. Vol. II. M. de Brabender, and J.D. Mey, editors. Elsevier, New York. 399–425.
7. Casal, J., C. González, and P. Ripoll. 1990. Spindles and centrosomes during male meiosis in *Drosophila melanogaster*. *Eur. J. Cell Biol.* 51:38–44.
8. Casal, J., C. González, F. Wandosell, J. Avila, and P. Ripoll. 1990. Abnormal meiotic spindles cause a cascade of defects during spermatogenesis in *asp* males of *Drosophila*. *Development*. 108:251–260.
9. Cavener, D.R., and S.C. Ray. 1991. Eukaryotic start and stop translation sites. *Nucleic Acids Res.* 19:3185–3192.
10. Churchill, M.E., and A.A. Travers. 1991. Protein motifs that recognize structural features of DNA. *Trends Biochem Sci*. 16:92–97.
11. Cooley, L., R. Kelley, and A. Spradling. 1988. Insertional mutagenesis of the *Drosophila* genome with single *P* elements. *Science*. 239:1121–1128.
12. Devereaux, J., P. Haeberli, and O. Smithies. 1984. A comprehensive set of sequence analysis programs for the VAX. *Nucleic Acids Res.* 12:387–395.
13. Endow, S.A., and M. Hatsumi. 1991. A multimember kinesin gene family in *Drosophila*. *Proc. Natl. Acad. Sci*. 88:4424–4427.
14. Enos, A.P., and N.R. Morris. 1990. Mutation of a gene that encodes a kinesin-like protein blocks nuclear division in *A. nidulans*. *Cell*. 60:1019–1027.
15. Foe, V. 1989. Mitotic domains reveal early commitment of cells in *Drosophila* development. *Development*. 107:1–22.
16. Fuller, M.T. 1995. Riding the polar winds: chromosomes motor down east. *Cell*. 81:5–8.
17. Gatti, M., and B.S. Baker. 1989. Genes controlling essential cell-cycle functions in *Drosophila melanogaster*. *Genes Dev*. 3:438–453.
18. Glover, D.M., M.H. Leibowitz, D.A. McLean, and H. Parry. 1995. Mutations in *aurora* prevent centrosome separation leading to the formation of monopolar spindles. *Cell*. 81:95–105.
19. González, C., J. Casal, and P. Ripoll. 1988. Functional monopolar spindles caused by mutation in *mgr*, a cell division gene of *Drosophila melanogaster*. *J. Cell Sci.* 89:39–47.
20. González, C., and D.M. Glover. 1994. Techniques for studying mitosis in *Drosophila*. *In* The Cell Cycle: A Practical Approach. R. Brookes and P. Fantes, editors. IRL, Oxford University Press, Oxford, UK. 143–175.
21. Heald, R., R. Tournebize, T. Blank, R. Sandaltzopoulos, P. Becker, A. Hyman, and E. Karsenti. 1996. Self-organization of microtubules into bipolar spindles around artificial chromosomes in *Xenopus* egg extracts. *Nature*. 382:420–425.
22. Heck, M.M.S., A. Pereira, P. Pesavento, Y. Yannoii, A.C. Spradling, and L.S.B. Goldstein. 1993. The kinesin-like protein KLP61F is essential for mitosis in *Drosophila*. *J. Cell Biol*. 123:665–679.
23. Heuer, J.G., K. Li, and T.C. Kaufman. 1995. The *Drosophila* homeotic target gene *centrosomin (cnn)* encodes a novel centrosomal protein with leucine zippers and maps to a genomic region required for midgut morphogenesis. *Development*. 121:209–218.
24. Kashina, A.S., R.J. Baskin, D.G. Cole, K.P. Wedaman, W.M. Saxton, and J.M. Scholey. 1996. A bipolar kinesin. *Nature*. 379:270–272.
25. Kashina, A.S., J.M. Scholey, J.D. Leszyk, and W.M. Saxton. 1996. An essential bipolar mitotic motor. *Nature*. 384:225.
26. Krieg, P.A., and D.A. Melton. 1987. *In vitro* RNA synthesis with SP6 RNA polymerase. *Methods Enzymol*. 155:397–415.
27. Lindsley, D.L., and G.G. Zimm. 1992. The Genome of *Drosophila melanogaster*. Academic Press, New York. 1–1133.
28. Lupas, A., D.M. Van, and J. Stock. 1991. Predicting coiled coils from protein sequences. *Science*. 252:1162–1164.
29. Mazia, D. 1961. Mitosis and the physiology of cell division. *In* The Cell. Vol. III. Jean Brachet and Alfred E. Mirsky, editors. Academic Press Inc. LTD, London. 77–412.
30. Mole-Bajer, J. 1975. The role of centrioles in the development of the astral spindle (newt). *Cytobios*. 13:117–140.
31. Moore, J.D., and S.A. Endow. 1996. Kinesin proteins: a phylum of motors for microtubule-based motility. *Bioessays*. 18:207–219.
32. Murphy, T.D., and G.H. Karpen. 1995. Interactions between the nod^+ kinesin-like gene and extra-centromeric sequences are required for transmission of a *Drosophila* minichromosome. *Cell*. 81:139–148.
33. Nangaku, M., R. Sato-Yoshitake, Y. Okada, Y. Noda, R. Takemura, H. Yamazaki, and N. Hirokawa. 1994. KIF1B, a novel microtubule plus end–directed monomeric motor protein for transport of mitochondria. *Cell*. 79:1209–1220.
34. Nigg, E.A. 1993. Cellular substrates of p34cdc2 and its companion cyclin-dependent kinases. *Trends Cell Biol*. 3:296–301.
35. Nomura, N., T. Nagase, N. Miyajima, T. Sazuka, A. Tanaka, S. Sato, N. Seiki, Y. Kawarabayasi, K. Ishikawa, and S. Tabata. 1994. Prediction of the coding sequences of unidentified human genes. II. The coding sequences of 40 new genes (KIAA0041-KIAA0080) deduced by analysis of cDNA clones from human cell line KG-1. *DNA Res. 1*. 1:223–229.
36. Ohkura, H., T. Torok, G. Tick, J. Hoheisel, I. Kiss, and D.M. Glover. 1997. Mutation of a gene for a *Drosophila* kinesin-like protein, *Klp38B,* leads to failure of cytokinesis. *J. Cell Sci.* 110:945–954.
37. Okada, Y., H. Yamazaki, Y. Sekine-Aizawa, and N. Hirokawa. 1995. The neuron-specific kinesin superfamily protein KIF1A is a unique monomeric motor for anterograde axonal transport of synaptic vesicle precursors. *Cell*. 81:769–780.
38. Piperno, G., and M.T. Fuller. 1985. Monoclonal antibodies specific for an acetylated form of α-tubulin recognize the antigen in cilia and flagella from a variety of organisms. *J Cell Biol*. 101:2085–2094.
39. Rattner, J.B., and M.W. Berns. 1976. Distribution of microtubules during centriole separation in rat kangaroo (*Protorous*) cells. *Cytobios.* 15:37–43.
40. Rieder, C.L., and S.P. Alexander. 1990. Kinetochores are transported poleward along a single astral microtubule during chromosome attachment to the spindle in newt lung cells. *J. Cell Biol.* 110:81–95.
41. Rieder, C.L., and E.D. Salmon. 1994. Motile kinetochores and polar ejection forces dictate chromosome position on the vertebrate mitotic spindle. *J. Cell Biol.* 124:223–233.
42. Rieder, C.L., E.A. Davison, L.C. Jensen, L. Cassimeris, and E.D. Salmon. 1986. Oscillatory movements of monooriented chromosomes and their position relative to the spindle pole result from the ejection properties of the aster and half-spindle. *J Cell Biol*. 103:581–591.
43. Ruden, D., W. Cui, V. Sollars, and M. Alterman. 1997. A *Drosophila* kinesin-like protein, Klp38B, functions during meiosis, mitosis, and segmentation. *Dev. Biol.* In press.
44. Sablin, E.P., F.J. Kull, R. Cooke, R.D. Vale, and R.J. Fletterick. 1996. Crystal structure of the motor domain of the kinesin-related motor ncd. *Nature*. 380:555–559.
45. Sambrook, J., E.F. Fritsch, and T. Maniatis. 1989. Molecular Cloning: A Laboratory Manual. Cold Spring Harbor Laboratory Press, Cold Spring Harbor, NY. 14.12–14.13.
46. Sunkel, C.E., and D.M. Glover. 1988. polo, a mitotic mutant of *Drosophila* displaying abnormal spindle poles. *J Cell Sci.* 89:25–38.
47. Theurkauf, W.E., and R.S. Hawley. 1992. Meiotic spindle assembly in *Drosophila* females: behavior of nonexchange chromosomes and the effects of mutations in the nod kinesin-like protein. *J Cell Biol*. 116:1167–1180.
48. Vernós, I., and E. Karsenti. 1995. Chromosomes take the lead in spindle assembly. *Trends Cell Biol*. 5:297–301.
49. Vernós, I., J. Raats, T. Hirano, J. Heasman, E. Karsenti, and C. Wylie. 1995. Xklp1, a chromosomal *Xenopus* kinesin-like protein essential for spindle organization and chromosome positioning. *Cell*. 81:117–127.
50. Wang, S.-Z., and R. Adler. 1995. Chromokinesin: a DNA-binding, kinesin-like nuclear protein. *J. Cell Biol.* 128:761–768.
51. Waters, J.C., R.W. Cole, and C.L. Rieder. 1993. The force-producing mechanism for centrosome separation during spindle formation in vertebrates is intrinsic to each aster. *J. Cell Biol.* 122:361–372.
52. Wilson, P.G., M.T. Fuller, and G.G. Borisy. 1997. Monastral bipolar spindles: implications for dynamic centrosome organization. *J. Cell Sci.* 110: 451–464.
53. Zhang, P., and R.S. Hawley. 1990. The genetic analysis of distributive segregation in *Drosophila melanogaster*. II. Further genetic analysis of the nod locus. *Genetics*. 125:115–127.
54. Zhang, P., B.A. Knowles, L.S. Goldstein, and R.S. Hawley. 1990. A kinesin-like protein required for distributive chromosome segregation in *Drosophila*. *Cell*. 62:1053–1062.